REVIEW
Korean J Intern Med 2012;27:1-12
http://dx.doi.org/10.3904/kjim.2012.27.1.1

pISSN 1226-3303 eISSN 2005-6648
http://www.kjim.or.kr

The Role of Optical Coherence Tomography in Coronary Intervention

Mitsuyasu Terashima[1], Hideaki Kaneda[2], and Takahiko Suzuki[1]

[1]Department of Cardiology, Toyohashi Heart Center, Toyohashi; [2]Okinaka Memorial Institute for Medical Research, Tokyo, Japan

Optical coherence tomography (OCT) is an optical analog of intravascular ultrasound (IVUS) that can be used to examine the coronary arteries and has 10-fold higher resolution than IVUS. Based on polarization properties, OCT can differentiate tissue characteristics (fibrous, calcified, or lipid-rich plaque) and identify thin-cap fibroatheroma. Because of the strong attenuation of light by blood, OCT systems required the removal of blood during OCT examinations. A recently developed frequency-domain OCT system has a faster frame rate and pullback speed, making the OCT procedure more user-friendly and not requiring proximal balloon occlusion. During percutaneous coronary intervention (PCI), OCT can provide detailed information (dissection, tissue prolapse, thrombi, and incomplete stent apposition [ISA]). At follow-up examinations after stent implantation, stent strut coverage and ISA can be assessed. Several OCT studies have demonstrated delayed neointimal coverage following drug-eluting stent (DES) implantation vs. bare metal stent (BMS) placement. While newer DESs promote more favorable vascular healing, the clinical implications remain unknown. Recent OCT studies have provided insights into restenotic tissue characteristics; DES restenotic morphologies differ from those with BMSs. OCT is a novel, promising imaging modality; with more in-depth assessments of its use, it may impact clinical outcomes in patients with symptomatic coronary artery disease.

Keywords: Tomography, optical coherence; Ultrasonography, interventional; Angioplasty; Stents; Coronary disease

INTRODUCTION

Optical coherence tomography (OCT) is a method of obtaining tomographic images of a human organ based on the coherence of light. Around 1990, OCT was independently developed by two Japanese researchers, Naohiro Tanno of Yamagata University, Japan, and James G. Fujimoto of the Massachusetts Institute of Technology (MIT) in the United States, and patent applications were submitted at about the same time in Japan and the United States during 1991. *In vitro* observation of the retina and coronary artery was first performed in 1991 [1]. OCT was initially applied in the clinical setting in the ophthalmology field in 1996 and is now widely used to assess retinal diseases and other conditions.

In cardiology, OCT is an optical analog of intravascular ultrasound (IVUS), used to examine the coronary arteries. Ultrasound employed for IVUS examination is replaced by near-infrared light with a wavelength of about 1,300 nm, which is absorbed by red blood cells, water, lipids, and protein at relatively low levels. Through a rotating glass fiber-optic system, coherent infrared light can be directed

Received : October 3, 2011
Accepted: October 5, 2011

Correspondence to Mitsuyasu Terashima, M.D.
Department of Cardiology, Toyohashi Heart Center, 21-1 Gobudori, Oyama-cho, Toyohashi 441-8530, Japan
Tel: 81-532-37-3377, Fax: 81-532-37-3366, E-mail: mterashima-circ@umin.ac.jp

Copyright © 2012 The Korean Association of Internal Medicine
This is an Open Access article distributed under the terms of the Creative Commons Attribution Non-Commercial License (http://creativecommons.org/licenses/by-nc/3.0/) which permits unrestricted non-commercial use, distribution, and reproduction in any medium, provided the original work is properly cited.

Table 1. Comparison of IVUS and first-generation time-domain OCT

Specifications	IVUS	First-generation OCT
Axial resolution, μm	100-150	10-20
Lateral resolution, μm	150-300	25-40
Frame rate, fps	30	15-20
Pullback speed, mm/sec	0.5-2.0	0.5-2.0
Scan diameter (FOV), mm	8-10	6.8
Tissue penetration, mm	4-8	1-2
Balloon occlusion	Not necessary	Highly recommended

IVUS, intravascular ultrasound; OCT, optical coherence tomography; fps, frames per second; FOV, field of view.

and reflected within the tissue to create a detailed tissue image with extraordinarily high resolution, and IVUS-like cross-sectional tomographic images can be obtained. OCT and IVUS differ in several respects, as shown in Table 1. The resolution of OCT (to 10-20 μm) is about 10-fold higher than that of IVUS (to 100-150 μm), but the maximum depth of tissue penetration is lower with OCT (1-2 mm) than with IVUS (4-8 mm). Another important difference is related to the strong attenuation of light by blood, which originates from two sources: absorption by hemoglobin and scattering by red blood cells. To examine coronary arteries, blood must first be removed during an OCT examination to eliminate massive scattering of light by red blood cells.

OCT SYSTEM AND TECHNIQUE

Time-domain OCT

The first clinically/commercially available OCT system in the cardiology field was produced by LightLab Imaging Inc. (Westford, MA, USA). The first-generation OCT (ImageWire and M2/3 OCT system; LightLab Imaging Inc.) incorporated both an OCT imaging wire and an over-the-wire occlusion balloon. First, a conventional 0.014″ angioplasty guide wire is used to cross the lesion and an occlusion balloon is passed along the guide wire beyond the lesion. Then, the guide wire and the imaging wire are exchanged. To examine the lesion, the occlusion balloon is pulled back proximal to the lesion and then dilated at a low pressure to block blood flow. Blood is then removed by flushing with lactated Ringer's solution or normal saline. In our experience, symptoms and electrocardiographic changes often persist when normal saline is used for flushing. Thus, we recommend the use of lactated Ringer's solution. Advancing the occlusion balloon across a severe stenosis is occasionally difficult. In such cases, a skilled operator may cross an imaging wire alone across the severe stenosis, and then dilate the occlusion balloon proximal to the lesion.

We conducted a multicenter study to evaluate the safety and efficacy of the first-generation OCT in comparison with IVUS, which revealed an average duration of vascular obstruction of 48.3 ± 14.7 seconds with no serious complication due to the procedure, including coronary artery dissection, embolism, severe arrhythmia (such as ventricular tachycardia or ventricular fibrillation), or myocardial infarction [2]. Additionally, OCT imaging was superior to IVUS for the visualization of the lumen border. Of note, the OCT image wire was able to cross five of six tight lesions that the IVUS catheter was unable to cross.

Although the first-generation OCT had the disadvantage of requiring a more complex procedure (i.e., balloon occlusion) than required with the IVUS, as described above, a more convenient method to remove blood was recently introduced. Kataiwa et al. [3] and Prati et al. [4] reported that blood could be removed by flushing with low-molecular-weight dextran or contrast medium through a guide catheter instead of requiring an occlusion balloon for observation.

Frequency-domain OCT

The first-generation OCT system was based on a time-domain OCT (TD-OCT) imaging method that relies on a moving reference mirror to scan each depth position in the image pixel. This mechanical scanning process limits the rate at which images can be acquired (Fig. 1A). To overcome this limitation, a new generation of OCT systems that employ frequency-domain OCT imaging methods has been developed [5,6]. These systems are known as

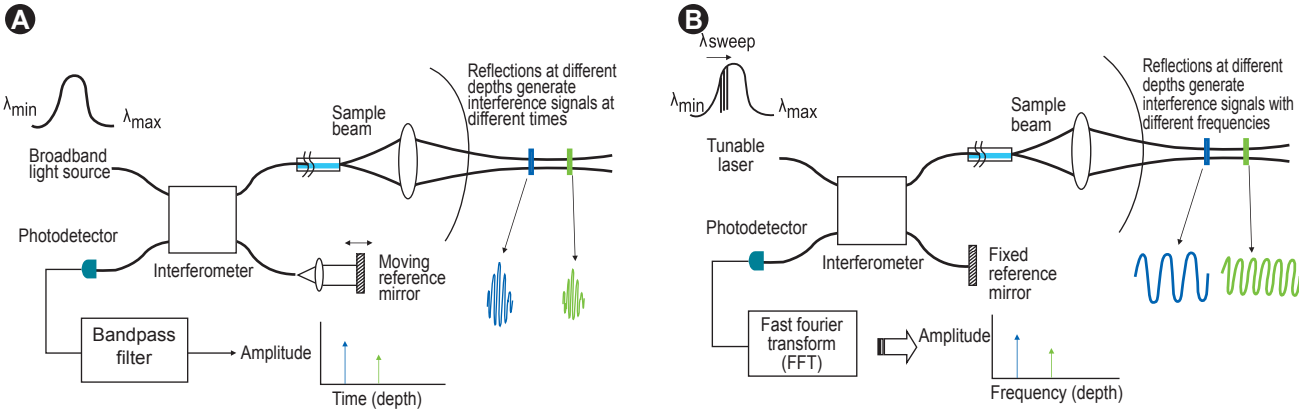

Figure 1. (A) Time-domain optical coherence tomography system. (B) Fourier/frequency-domain optical coherence tomography system.

Table 2. Comparison of TD-OCT and FD-OCT

Specifications	M3 (TD-OCT)	C7-XR (FD-OCT)
Axial resolution, μm	15-20	12-15
Lateral resolution, μm	39	19
Frame rate, fps	20	100
Lines/frame	240	500
Pullback speed, mm/sec	0.5-2.0	10-25
Scan diameter (FOV), mm	6.8	10
Tissue penetration, mm	1-2	1-2
Balloon occlusion	Highly recommended	Optional

OCT, optical coherence tomography; TD, time-domain; FD, frequency-domain; fps, frames per second; FOV, field of view.

frequency-domain OCT (FD-OCT), Fourier-domain OCT, swept-source OCT (SS-OCT), or optical frequency-domain imaging (OFDI). In FD-OCT imaging methods, interferometric data are measured as a function of optical wavelength and time, rather than as a function of time alone, based on the introduction of a fixed reference mirror and a tunable laser light source with a sweep range of 1,250-1,370 nm, instead of the broadband light source used in TD-OCT imaging systems (Fig. 1B). This imaging method enables much faster image acquisition rates and pullback speeds, resulting in a simpler, non-occlusive OCT imaging approach with flushing of viscous contrast through the guide catheter to remove blood from the artery [7].

Recently, a commercially available FD-OCT system has been developed (Dragonfly imaging catheter and C7-XR OCT system; LightLab Imaging, Inc.). Differences between TD- (M3) and FD-OCT (C7-XR) systems are shown in Table 2. For FD-OCT imaging using the Dragonfly imaging catheter, a ≥ 6-Fr-diameter guide catheter is recommended. Viscous iso-osmolar contrast media or low-molecular-weight dextrose can be used for non-occlusive flushing, although higher-viscosity solutions have been found to provide superior results. The OCT imaging catheter is advanced distally into the coronary artery via a standard angioplasty guide wire (0.014″). As with the non-occlusive TD-OCT technique, care should be taken to position the guide catheter coaxially and deeply into the coronary ostium. Automated intravascular OCT pullback is performed during contrast injection through the guide catheter, either automatically with a power injector (typical flush rate 3.0 mL/sec) or manually with a syringe.

A recent study showed that FD-OCT is a feasible and safe technique for the guidance of coronary interventions (see below) [3,7,8]. Larger randomized studies will confirm whether the use of FD-OCT can improve clinical outcomes.

EXAMINATION OF CORONARY ARTERY LESIONS AND OCT PLAQUE CHARACTERISTICS

Due to its high resolution (10-15 μm), OCT can differentiate the internal and external elastic laminae, as well as distinguish the intima/media/adventitia, which is impossible with the low resolution (100-150 μm) of IVUS [9]. OCT can also differentiate tissue characteristics based on polarization properties. High birefringence by polarization shift identifies fibrous tissue, collagen, and lipid composition. Low birefringence reflects calcium. By overlying low and high birefringent images on the OCT image map, tissue structures can be highlighted by tissue composition. In a comparison using autopsy specimens, Yabushita et al. [10] reported that OCT images of each type of plaque had the following features: 1) fibrous plaque: a homogenous high-signal region with low attenuation; 2) calcified plaque: a well-delineated, low-signal region with sharp borders; and 3) lipid-rich plaque: a low-signal region with diffuse borders. They reported > 90% sensitivity and specificity for detecting lipid-rich plaque, based on comparisons with pathological specimens. In another study, Kume et al. [11] also concluded that OCT had a high sensitivity for detecting lipid-rich plaque.

DIAGNOSIS OF UNSTABLE PLAQUE

In addition to its ability to detect lipid-rich plaque, as mentioned above, the high resolution of OCT makes it possible to identify a very thin (< 100 μm) fibrous cap covering a lipid core, which is difficult to detect with other modalities [12]. Autopsy studies demonstrated that fibroatheroma with a thin fibrous cap of < 65 μm (thin-cap fibroatheroma [TCFA]) is often found in culprit lesions in acute coronary syndromes (ACSs) and is considered to be a vulnerable plaque [13]. Early diagnosis of TCFAs may lead to more aggressive medical/invasive treatment of symptomatic and asymptomatic coronary artery disease to improve prognosis and clinical outcomes.

OCT-derived TCFA was defined as a lipid-rich plaque (lipid arc within a plaque in ≥ 2 quadrants) with a thin fibrous cap (thickness at the thinnest segment < 65 μm) (Fig. 2) [14]. Our OCT examination of a patient with ACS revealed ruptured plaque with a thin fibrous cap at the site of a culprit lesion that could not be detected by IVUS (Fig. 3). Kubo et al. [15] assessed culprit lesions in patients with acute myocardial infarction by OCT, IVUS, and coronary angioscopy, and reported that OCT was the most sensitive imaging modality for detecting the rupture and erosion of culprit plaque, and most frequently detected TCFAs. Additionally, OCT can distinguish between red and white thrombi using differences in the signal attenuation curve, which are frequently observed in unstable plaque [16].

Moreover, OCT may be able to assess inflammatory cell infiltration, primarily active macrophages, another characteristic of unstable plaque. Based on OCT examination, MacNeill et al. [17] reported that plaque in patients with ACS had a high density of macrophages, and that this density was higher in ruptured plaque than in non-ruptured plaque.

While many authors have reported on the usefulness of OCT for tissue characterization, as indicated above, Manfrini et al. [18] performed a comparison with pathological findings and found that the detection rates by OCT

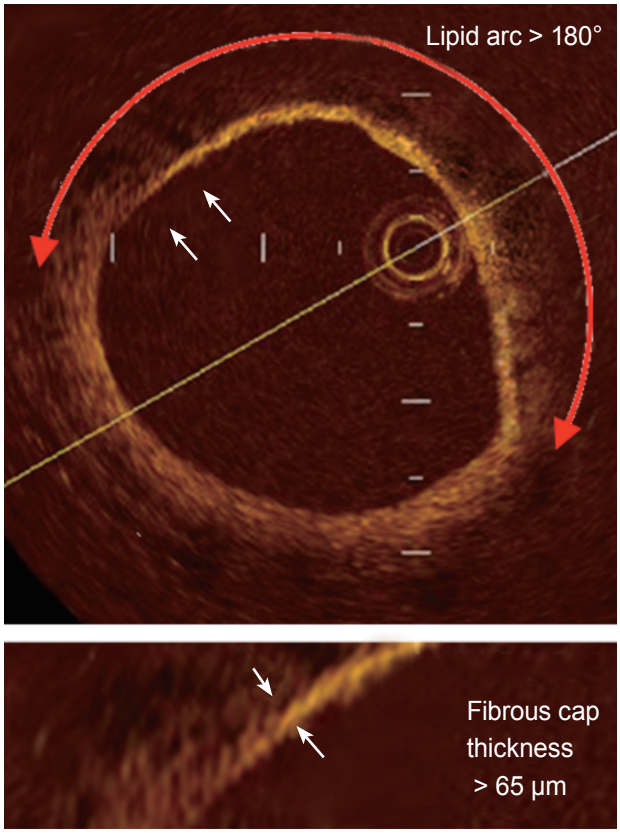

Figure 2. Optical coherence tomography-derived thin-cap fibroatheroma was defined as a lipid-rich plaque (lipid arc within a plaque in ≥ 2 quadrants) with a thin fibrous cap (thickness at the thinnest segment < 65 μm).

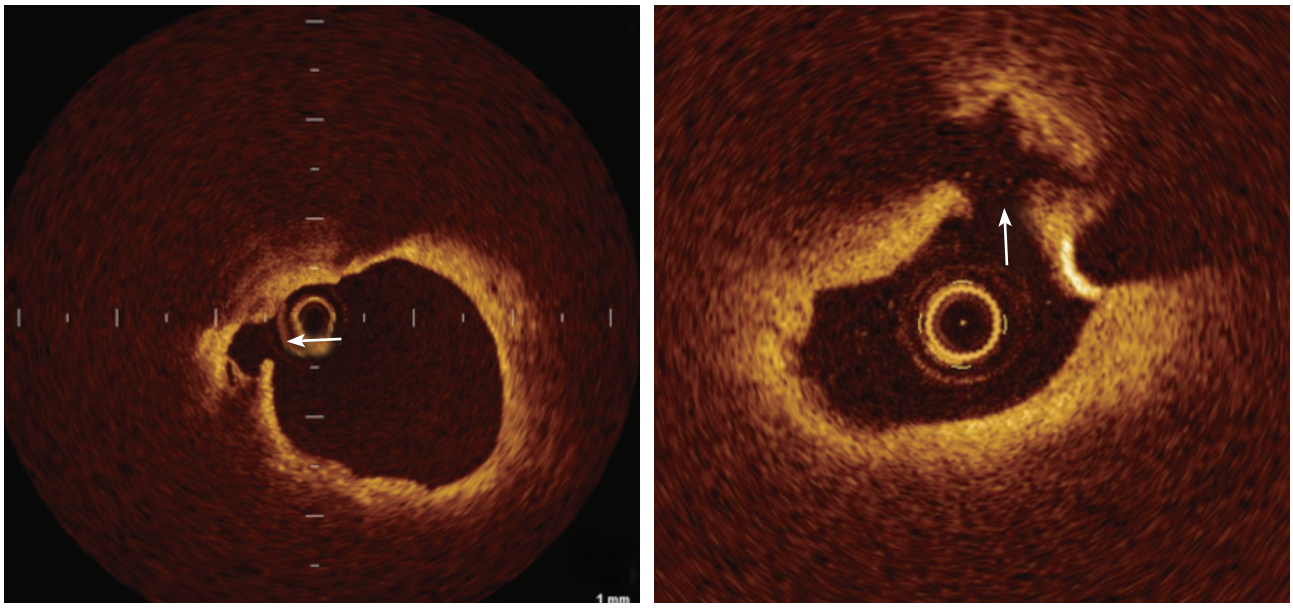

Figure 3. Optical coherence tomography image of ruptured plaque (arrows) with a thin fibrous cap at the site of an acute coronary syndrome culprit lesion.

differed for each type of plaque (45% for fibrous-cap atheroma, 68% for fibrocalcific plaque, and 83% for fibrous plaque). They suggested that the low detection rates for fibrous-cap atheroma and fibrocalcific plaque may be due to the inability to detect the lipid core and calcium deposits located behind a thick fibrous cap because of the low tissue penetration of OCT, and that the lipid core and calcium deposits were both seen as low-intensity areas that were difficult to distinguish. Low tissue penetration is a fundamental limitation of the current system. Moreover, distinguishing lipid from calcium is a subjective process and its precision could depend on the skill of the observer, as is the case for gray-scale IVUS. Thus, establishing objective diagnostic criteria is desirable.

APPLICATION OF OCT IN PERCUTANEOUS CORONARY INTERVENTION (PCI)

Because OCT has a high resolution, it can provide detailed information about the vessel that cannot be obtained with other modalities. Example cases are shown in Figs. 4 and 5. The case depicted in Fig. 4 demonstrated spontaneous dissection that could not be found on angiography or IVUS. Fig. 5 shows an example of a cutting balloon angioplasty. Multiple tears in the intima were observed after dilatation with a cutting balloon that also could not be detected by angiography or IVUS. Thus, this technology offers detailed visualization of vessel injury after stent implantation, such as tissue prolapse, dissections, and thrombus, and enables systematic classification and quantification *in vivo* [19,20].

After implantation of a drug-eluting stent (DES), not only dissection, tissue prolapse, and thrombi, but also incomplete stent apposition (ISA), have attracted attention in relation to stent thrombosis and should be assessed in detail [19]. When assessing ISA, we should recall that the near-infrared light used in OCT does not penetrate metal stent struts, similar to IVUS. The stent strut is visualized as a linear structure with strong surface reflection and typical dorsal shadowing, and the posterior side of each strut near the vessel wall cannot be observed (Fig. 6) [21,22]. Thus, it is necessary to determine whether the strut has made an indentation on the intimal surface of the vessel (Fig. 6A) or to measure the distance between the surface reflection of the strut and the adjacent visible vessel surface while taking the thickness of the strut into account (Fig. 6B). To ensure the accurate assessment of ISA, we validated the accuracy of OCT measurement of the strut thickness of several commercially available stents *in vitro*. Differences in OCT stent strut measurements as compared with the manufacturers' nominal strut thick-

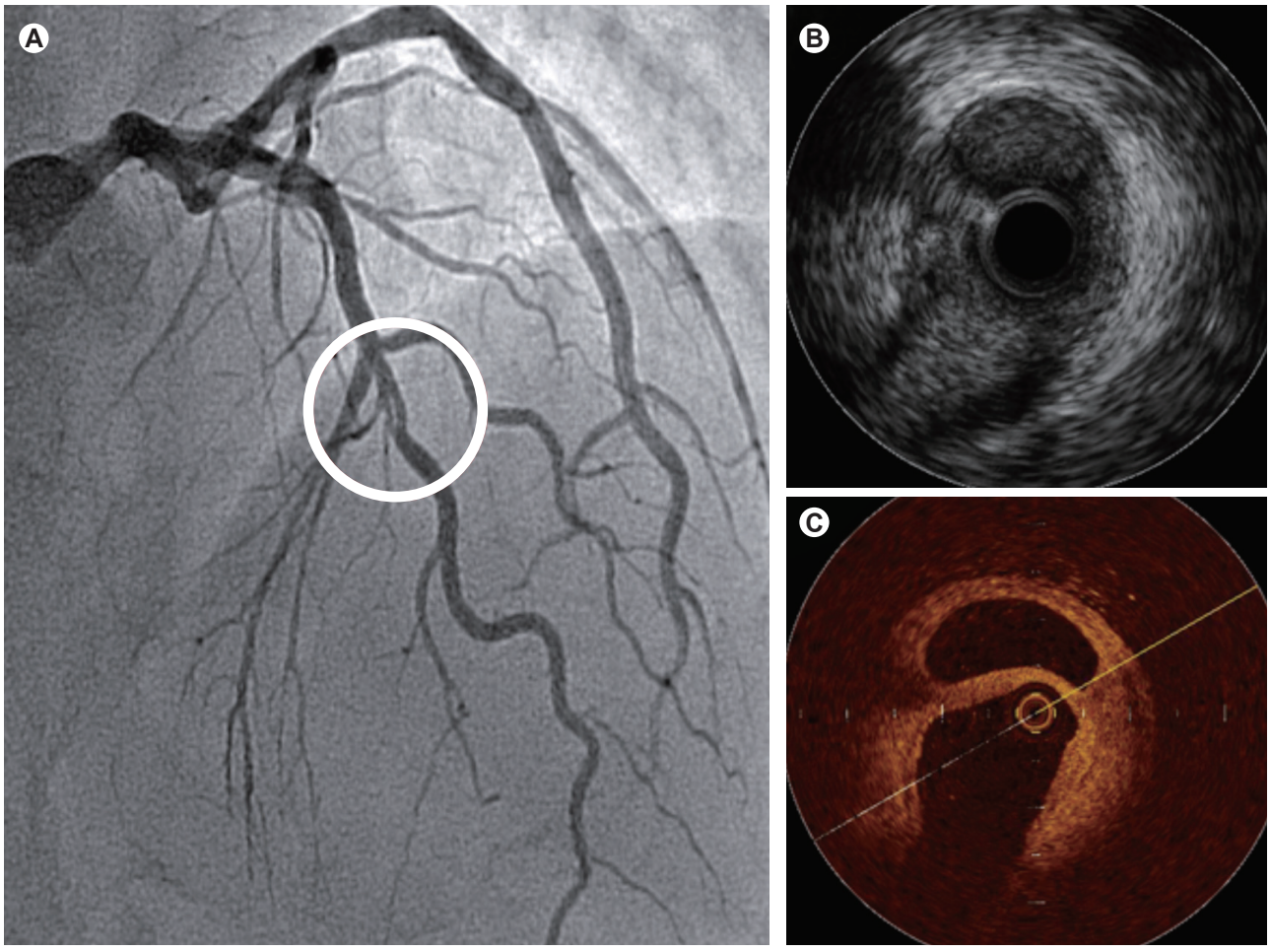

Figure 4. A case with spontaneous dissection. Optical coherence tomography (C) visualized spontaneous dissection that could not be found with angiography (A) or intravascular ultrasound (B).

ness data were small and reproducibility of the measurements was high, suggesting that the assessment of stent strut apposition using OCT is feasible [21].

As described above, the capability of OCT to examine the structure of the arterial wall before or after PCI is superior to those of other imaging modalities, such as angiography and IVUS, and the application of OCT during PCI seems logical and promising, yet the assessment of clinical significance to date has been limited to observations and has not necessarily included clinical outcomes. Furthermore, OCT has several inherent limitations. Given its limited penetration depth and/or scan range, the whole-vessel structure of a lesion with a large plaque burden or a large vessel cannot be visualized. Additionally, first-generation TD-OCT also requires displacement of the blood during imaging with balloon occlusion methods, making the PCI procedure more complex and precluding the use of this technique for ostial lesions, including the left main coronary artery (lesions). As the newly developed FD-OCT system does not require coronary artery occlusion and has a faster pullback speed [5,6], it may be more suitable for PCI. The clinical significance of OCT for PCI needs to be further established in larger-scale clinical trials.

OCT FOLLOW-UP EXAMINATIONS AFTER PCI

Stent strut coverage and ISA

DESs significantly suppress neointimal hyperplasia. A study of OCT and IVUS demonstrated that two-thirds of sirolimus-eluting stent (SES) struts are covered by neointi-

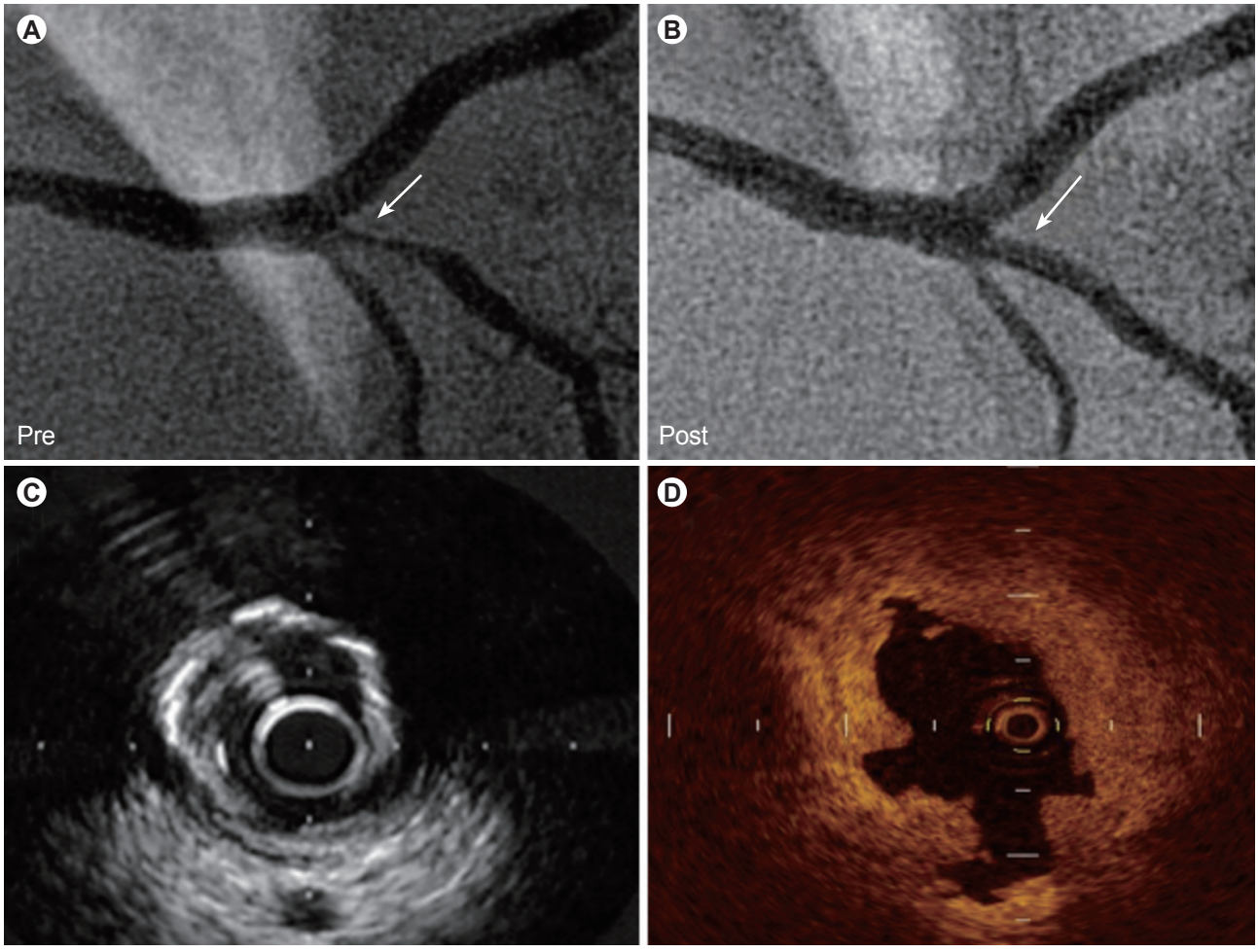

Figure 5. A case with cutting balloon angioplasty. Cutting balloon angioplasty was performed for stenosis in the right posterior descending artery (A, arrow). Multiple tears in the intima were observed after dilatation with a cutting balloon on the optical coherence tomographic image (D), which could not be detected by angiography (B, arrow) or intravascular ultrasound (C).

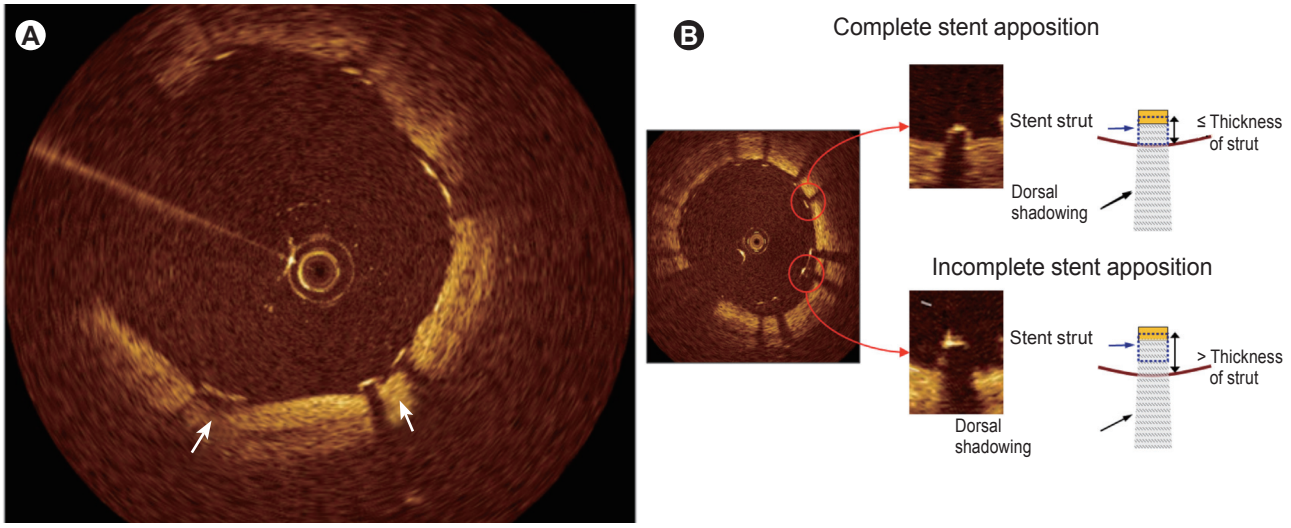

Figure 6. Identification of stent apposition. The stent is visualized as a linear structure with strong surface reflection and typical dorsal shadowing, and the posterior side of each strut near the vessel wall cannot be observed. Thus, it is necessary to determine whether the strut has made an indentation on the intimal surface of the vessel (A) or to measure the distance between the surface reflection of the strut and the adjacent visible vessel surface while taking the thickness of the strut into account (B).

ma < 100 μm in thickness, which is beyond the resolution of IVUS [23]. Thus, OCT is most useful for examining patients at follow-up after DES implantation, and is capable of detecting a thin neointima due to its high resolution (Fig. 7). In recent years, late stent thrombosis in patients treated with DES has become a major concern. Delayed coverage or failure to cover an exposed stent with neointima/regenerated endothelium has been suggested as a cause of thrombosis.

Both OCT and angioscopy have been recognized as useful methods for *in vivo* assessment of the intimal coverage of a stent. Although angioscopy provides a wide-angle forward view, anatomical structures, such as tortuous vessels, may prohibit a complete circumferential view. While angioscopy allows direct observation of the vascular lumen and endothelial surface, the internal structure of the vessel wall cannot be assessed. Given these disadvantages of angioscopy, OCT may offer better quantitative performance for assessments. Thus, longitudinal/serial OCT studies (pre/post-intervention vs. follow-up) have been performed to evaluate the tissue coverage response of the artery to stent implantation [23-26].

Several classifications of tissue coverage of a stent strut are available [24,27]. In 2006, we proposed the OCT classification of tissue coverage of struts shown in Fig. 8 [28,29]. Although consensus on the definitions of the tissue coverage of stent struts has not yet been obtained, our classification is similar to that of Guagliumi and Sirbu [27]. The stent struts were usually assessed at 1-mm intervals, and strut, cross-section/frame, and stent/patient-base analyses were performed. Observations of struts in the same stent are not independent of one another. Using OCT, many papers demonstrated a delay in neointimal coverage following DES implantation in comparison with that of bare metal stents (BMSs), corresponding to pathological data. In comparisons among different kinds of DESs, second-generation DESs (zotarolimus-eluting [Endeavor, Medtronic CardioVascular, Santa Rosa, CA, USA] or everolimus-eluting [Xience V, Abbott Vascular Devices, Abbott Park, IL, USA; Promus, Boston Scientific, Natick, MA, USA]) demonstrated more favorable vascular healing following stent implantation, better neointimal coverage, and less ISA than did first-generation DESs (sirolimus-eluting [Cypher, Cordis Johnson & Johnson, Hialeah, FL, USA] or paclitaxel-eluting [TAXUS, Boston Scientific] stents) [25,30-32]. Furthermore, the healing processes are delayed in patients with ACS (especially ST-segment-elevation myocardial infarction) in comparison with patients with stable angina pectoris [33-35]. Stent overlapping or bifurcation/branching also affects stent strut coverage [36-39].

Thus, it is expected that detailed findings obtained by

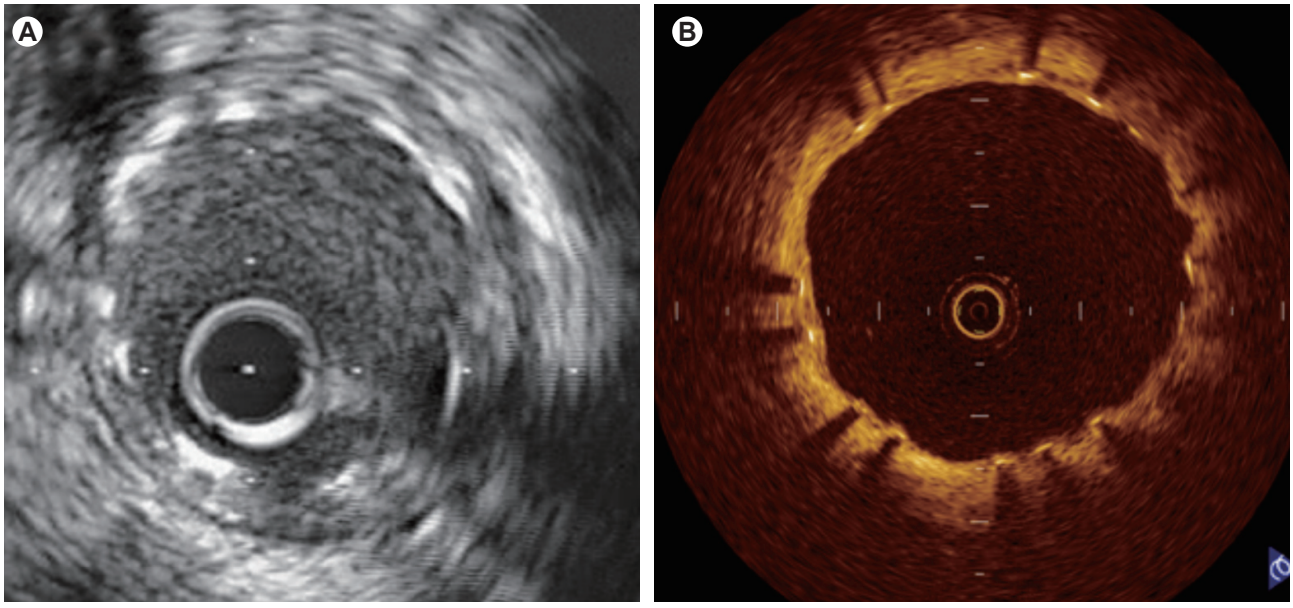

Figure 7. Intravascular ultrasonic (IVUS) and optical coherence tomographic (OCT) images obtained at 7 months after implantation of a drug-eluting stent (Cypher; 3.0 × 18 mm). While no obvious intimal growth is observed on the IVUS image (A), the OCT image (B) shows that the stent strut is covered by a very thin neointima (~100 μm).

OCT will be able to determine the characteristics of the neointima after various types of DES implantation, factors contributing to restenosis or thrombosis of DESs, and the proper use and appropriate duration of antiplatelet therapy after DES placement.

Restenotic tissue characteristics

OCT provides new insights into the characteristics of the tissue covering the stent struts. Several papers have reported OCT patterns of restenotic tissue components. A typical restenotic tissue of BMS at early follow-up (to 1 year), recognized as neointimal hyperplasia primarily composed of smooth muscle cells, is visualized as a homo-

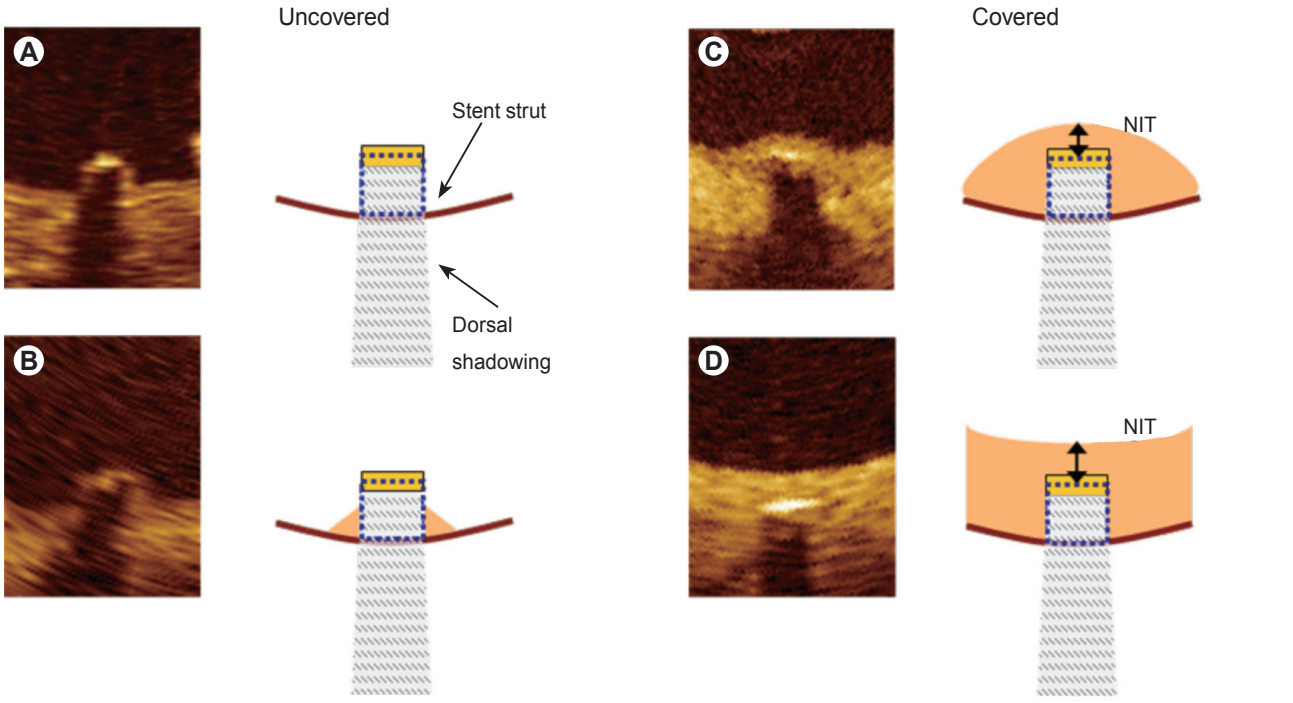

Figure 8. Classification of tissue coverage of stent struts. The left images (A, B) show uncovered struts and the right images (C, D) show covered struts. A strut with surrounding tissue beyond the strut surface is defined as covered. According to the shape of the tissue covering the struts, a covered strut is classified as convex (C) or embedded (D). The intimal thickness (NIT) was measured from the surface of the neointima covering the strut to the center line of the reflection.

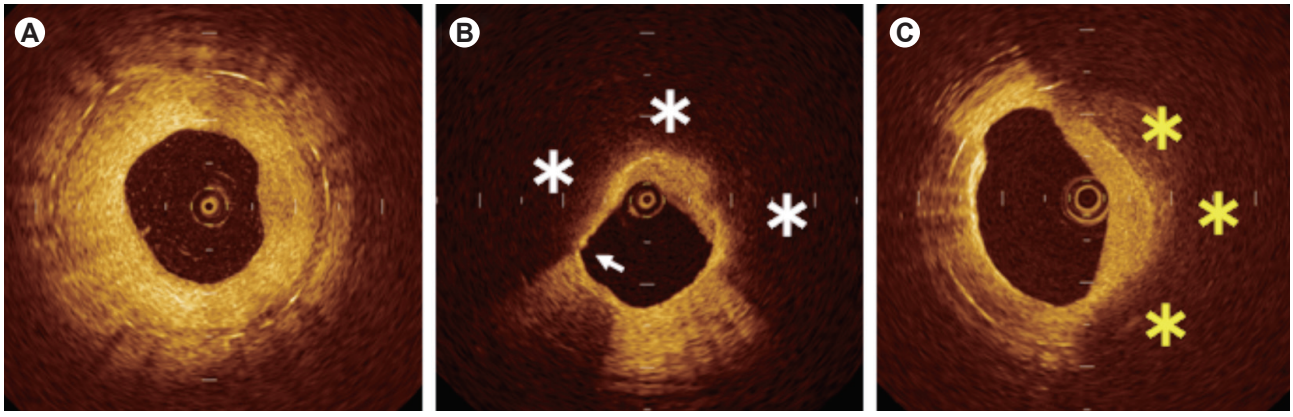

Figure 9. Optical coherence tomographic patterns of restenotic tissue following bare metal stent implantation. Homogeneous (A) and heterogeneous (B, C) intima. Lipid accumulation is suggested in the low-signal area with a diffuse lumen border within the area of neointimal hyperplasia (* in B), and calcification in the low-signal area with a sharp lumen border (* in C).

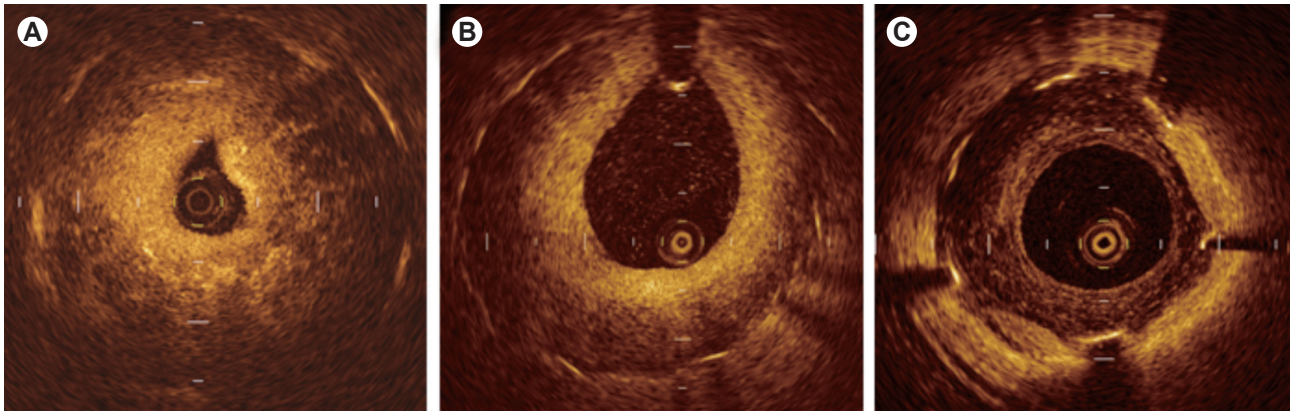

Figure 10. Optical coherence tomographic patterns of restenotic tissue following drug-eluting stent implantation. Patchy (A), layered (B), and speckled (C) patterns.

geneous structure by OCT (Fig. 9A) [40]. We have, however, reported that the characteristics of restenotic tissue in the very late phase (> 5 years) is frequently demonstrated as a heterogeneous structure suggesting lipid accumulation/calcification (Fig. 9B and 9C), occasionally accompanied by disruption of the intima, microvessels within neointima, or intraluminal materials [41]. The restenotic tissue of DESs, even in an early phase, also demonstrates polymorphic patterns in structure, backscatter, and composition (Fig. 10) [42,43]. This variation in OCT images could be caused by diverse components, including mature/immature smooth muscle cells and persistent fibrin or extracellular matrix, such as proteoglycans [43]. Thus, OCT provides important information about the tissue covering the stent struts. However, few studies have sought to validate OCT findings in comparison with pathological findings, and further investigations should be conducted until the impact of these findings on clinical outcomes is known.

FUTURE DIRECTIONS

As described above, OCT is a novel, promising imaging modality with characteristics that differ from those of traditional modalities, such as IVUS and angioscopy. However, OCT does not yet have the established clinical profile or ease-of-use of IVUS. As described, the advent of next-generation OCT, FD-OCT, is expected to make the procedure easier and faster. Since OCT has received more attention in Korea, Japan, China, and Europe, increasing numbers of OCT studies are being reported. Through these studies, we hope that the clinical role of OCT in PCI will be clarified in the future. We believe that the clinical usefulness of FD-OCT is likely to be greater than that of standard/previous-generation TD-OCT.

CONCLUSIONS

OCT is an imaging modality that can be expected to become increasingly popular in the future for the diagnosis and treatment of patients with symptomatic/asymptomatic coronary artery disease.

Conflict of interest

No potential conflict of interest relevant to this article was reported.

Acknowledgments

We thank Heidi N. Bonneau, RN, MS, CCA, for her review of the manuscript.

REFERENCES

1. Huang D, Swanson EA, Lin CP, et al. Optical coherence tomography. Science 1991;254:1178-1181.
2. Yamaguchi T, Terashima M, Akasaka T, et al. Safety and feasibility of an intravascular optical coherence tomography image wire system in the clinical setting. Am J Cardiol 2008;101:562-567.

3. Kataiwa H, Tanaka A, Kitabata H, et al. Head to head comparison between the conventional balloon occlusion method and the non-occlusion method for optical coherence tomography. Int J Cardiol 2011;146:186-190.
4. Prati F, Cera M, Ramazzotti V, et al. From bench to bedside: a novel technique of acquiring OCT images. Circ J 2008;72:839-843.
5. Barlis P, Schmitt JM. Current and future developments in intracoronary optical coherence tomography imaging. EuroIntervention 2009;4:529-533.
6. Takarada S, Imanishi T, Liu Y, et al. Advantage of next-generation frequency-domain optical coherence tomography compared with conventional time-domain system in the assessment of coronary lesion. Catheter Cardiovasc Interv 2010;75:202-206.
7. Imola F, Mallus MT, Ramazzotti V, et al. Safety and feasibility of frequency domain optical coherence tomography to guide decision making in percutaneous coronary intervention. EuroIntervention 2010;6:575-581.
8. Templin C, Meyer M, Muller MF, et al. Coronary optical frequency domain imaging (OFDI) for in vivo evaluation of stent healing: comparison with light and electron microscopy. Eur Heart J 2010;31:1792-1801.
9. Jang IK, Bouma BE, Kang DH, et al. Visualization of coronary atherosclerotic plaques in patients using optical coherence tomography: comparison with intravascular ultrasound. J Am Coll Cardiol 2002;39:604-609.
10. Yabushita H, Bouma BE, Houser SL, et al. Characterization of human atherosclerosis by optical coherence tomography. Circulation 2002;106:1640-1645.
11. Kume T, Akasaka T, Kawamoto T, et al. Assessment of coronary arterial plaque by optical coherence tomography. Am J Cardiol 2006;97:1172-1175.
12. Kume T, Akasaka T, Kawamoto T, et al. Measurement of the thickness of the fibrous cap by optical coherence tomography. Am Heart J 2006;152:755.e1-755.e4.
13. Virmani R, Kolodgie FD, Burke AP, Farb A, Schwartz SM. Lessons from sudden coronary death: a comprehensive morphological classification scheme for atherosclerotic lesions. Arterioscler Thromb Vasc Biol 2000;20:1262-1275.
14. Jang IK, Tearney GJ, MacNeill B, et al. In vivo characterization of coronary atherosclerotic plaque by use of optical coherence tomography. Circulation 2005;111:1551-1555.
15. Kubo T, Imanishi T, Takarada S, et al. Assessment of culprit lesion morphology in acute myocardial infarction: ability of optical coherence tomography compared with intravascular ultrasound and coronary angioscopy. J Am Coll Cardiol 2007;50:933-939.
16. Kume T, Akasaka T, Kawamoto T, et al. Assessment of coronary arterial thrombus by optical coherence tomography. Am J Cardiol 2006;97:1713-1717.
17. MacNeill BD, Jang IK, Bouma BE, et al. Focal and multi-focal plaque macrophage distributions in patients with acute and stable presentations of coronary artery disease. J Am Coll Cardiol 2004;44:972-979.
18. Manfrini O, Mont E, Leone O, et al. Sources of error and interpretation of plaque morphology by optical coherence tomography. Am J Cardiol 2006;98:156-159.
19. Gonzalo N, Serruys PW, Okamura T, et al. Optical coherence tomography assessment of the acute effects of stent implantation on the vessel wall: a systematic quantitative approach. Heart 2009;95:1913-1919.
20. Kawamori H, Shite J, Shinke T, et al. The ability of optical coherence tomography to monitor percutaneous coronary intervention: detailed comparison with intravascular ultrasound. J Invasive Cardiol 2010;22:541-545.
21. Terashima M, Rathore S, Suzuki Y, et al. Accuracy and reproducibility of stent-strut thickness determined by optical coherence tomography. J Invasive Cardiol 2009;21:602-605.
22. Sawada T, Shite J, Negi N, et al. Factors that influence measurements and accurate evaluation of stent apposition by optical coherence tomography: assessment using a phantom model. Circ J 2009;73:1841-1847.
23. Matsumoto D, Shite J, Shinke T, et al. Neointimal coverage of sirolimus-eluting stents at 6-month follow-up: evaluated by optical coherence tomography. Eur Heart J 2007;28:961-967.
24. Katoh H, Shite J, Shinke T, et al. Delayed neointimalization on sirolimus-eluting stents: 6-month and 12-month follow up by optical coherence tomography. Circ J 2009;73:1033-1037.
25. Kim JS, Jang IK, Fan C, et al. Evaluation in 3 months duration of neointimal coverage after zotarolimus-eluting stent implantation by optical coherence tomography: the ENDEAVOR OCT trial. JACC Cardiovasc Interv 2009;2:1240-1247.
26. Tanaka N, Terashima M, Rathore S, et al. Different patterns of vascular response between patients with or without diabetes mellitus after drug-eluting stent implantation: optical coherence tomographic analysis. JACC Cardiovasc Interv 2010;3:1074-1079.
27. Guagliumi G, Sirbu V. Optical coherence tomography: high resolution intravascular imaging to evaluate vascular healing after coronary stenting. Catheter Cardiovasc Interv 2008;72:237-247.
28. Terashima M, Ito T, Katoh O, et al. Relationship between stent apposition pattern and neointimal coverage after Sirolimus-eluting stent implantation: analysis by optical coherence tomography (abstract). J Am Coll Cardiol 2006;47:13B.
29. Ito T, Terashima M, Takeda Y, et al. Optical coherence tomographic analysis of neointimal stent coverage in Sirolimus-eluting stent, compared with bare metal stent (abstract). J Am Coll Cardiol 2006;47:13B.

30. Kim JS, Jang IK, Kim JS, et al. Optical coherence tomography evaluation of zotarolimus-eluting stents at 9-month follow-up: comparison with sirolimus-eluting stents. Heart 2009;95:1907-1912.
31. Choi HH, Kim JS, Yoon DH, et al. Favorable neointimal coverage in everolimus-eluting stent at 9 months after stent implantation: comparison with sirolimus-eluting stent using optical coherence tomography. Int J Cardiovasc Imaging 2011 Mar 26 [Epub]. http://dx.doi.org/10.1007/s10554-011-9849-7.
32. Gutierrez-Chico JL, van Geuns RJ, Regar E, et al. Tissue coverage of a hydrophilic polymer-coated zotarolimus-eluting stent vs. a fluoropolymer-coated everolimus-eluting stent at 13-month follow-up: an optical coherence tomography substudy from the RESOLUTE All Comers trial. Eur Heart J 2011;32:2454-2463.
33. Takano M, Inami S, Jang IK, et al. Evaluation by optical coherence tomography of neointimal coverage of sirolimus-eluting stent three months after implantation. Am J Cardiol 2007;99:1033-1038.
34. Kubo T, Imanishi T, Kitabata H, et al. Comparison of vascular response after sirolimus-eluting stent implantation between patients with unstable and stable angina pectoris: a serial optical coherence tomography study. JACC Cardiovasc Imaging 2008;1:475-484.
35. Guagliumi G, Costa MA, Sirbu V, et al. Strut coverage and late malapposition with paclitaxel-eluting stents compared with bare metal stents in acute myocardial infarction: optical coherence tomography substudy of the Harmonizing Outcomes with Revascularization and Stents in Acute Myocardial Infarction (HORIZONS-AMI) Trial. Circulation 2011;123:274-281.
36. Tahara S, Bezerra HG, Sirbu V, et al. Angiographic, IVUS and OCT evaluation of the long-term impact of coronary disease severity at the site of overlapping drug-eluting and bare metal stents: a substudy of the ODESSA trial. Heart 2010;96:1574-1578.
37. Guagliumi G, Musumeci G, Sirbu V, et al. Optical coherence tomography assessment of in vivo vascular response after implantation of overlapping bare-metal and drug-eluting stents. JACC Cardiovasc Interv 2010;3:531-539.
38. Her AY, Lee BK, Shim JM, et al. Neointimal coverage on drug-eluting stent struts crossing side-branch vessels using optical coherence tomography. Am J Cardiol 2010;105:1565-1569.
39. Gutierrez-Chico JL, Regar E, Nuesch E, et al. Delayed coverage in malapposed and side-branch struts with respect to well-apposed struts in drug-eluting stents: in vivo assessment with optical coherence tomography. Circulation 2011;124:612-623.
40. Kume T, Akasaka T, Kawamoto T, et al. Visualization of neointima formation by optical coherence tomography. Int Heart J 2005;46:1133-1136.
41. Habara M, Terashima M, Nasu K, et al. Difference of tissue characteristics between early and very late restenosis lesions after bare-metal stent implantation: an optical coherence tomography study. Circ Cardiovasc Interv 2011;4:232-238.
42. Gonzalo N, Serruys PW, Okamura T, et al. Optical coherence tomography patterns of stent restenosis. Am Heart J 2009;158:284-293.
43. Nagai H, Ishibashi-Ueda H, Fujii K. Histology of highly echolucent regions in optical coherence tomography images from two patients with sirolimus-eluting stent restenosis. Catheter Cardiovasc Interv 2010;75:961-963.